Chemical Engineering Science 96 (2013) 33–41

Contents lists available at SciVerse ScienceDirect

Chemical Engineering Science

journal homepage: www.elsevier.com/locate/ces

Study of calcium carbonate and sulfate co-precipitation

Y. Zarga [a], H. Ben Boubaker [a], N. Ghaffour [b,*], H. Elfil [a]

[a] LabTEN—Water Technologies Research Center, Technopole of Borj-Cédria, Tunisia
[b] Water Desalination and Reuse Center, King Abdullah University of Science and Technology (KAUST), KAUST P.O. Box 4700, ZC 23955-6900, Thuwal, Saudi Arabia

HIGHLIGHTS

- $CaCO_3$ and sulfate co-precipitation was investigated in this paper.
- Co-precipitation kinetics were studied by monitoring different parameters.
- $CaCO_3$ germination followed by gypsum (and vice-versa) precipitation was studied.
- The influence of co-precipitation ions was also investigated.

ARTICLE INFO

Article history:
Received 12 November 2012
Received in revised form
13 February 2013
Accepted 13 March 2013
Available online 4 April 2013

Keywords:
Precipitation
Nucleation
Kinetics
Fouling
Gypsum
Supersaturation

ABSTRACT

Co-precipitation of mineral based salts in scaling is still not well understood and/or thermodynamically well defined in the water industry. This study focuses on investigating calcium carbonate ($CaCO_3$) and sulfate mixed precipitation in scaling which is commonly observed in industrial water treatment processes including seawater desalination either by thermal-based or membrane-based processes. Co-precipitation kinetics were studied carefully by monitoring several parameters simultaneously measured, including: pH, calcium and alkalinity concentrations as well as quartz microbalance responses. The $CaCO_3$ germination in mixed precipitation was found to be different than that of simple precipitation. Indeed, the co-precipitation of $CaCO_3$ germination time was not anymore related to supersaturation as in a simple homogenous precipitation, but was significantly reduced when the gypsum crystals appeared first. On the other hand, the calcium sulfate crystals appear to reduce the energetic barrier of $CaCO_3$ nucleation and lead to its precipitation by activating heterogeneous germination. However, the presence of $CaCO_3$ crystals does not seem to have any significant effect on gypsum precipitation. IR spectroscopy and the Scanning Electronic Microscopy (SEM) were used to identify the nature of scales structures. Gypsum was found to be the dominant precipitate while calcite and especially vaterite were found at lower proportions. These analyses showed also that gypsum crystals promote calcite crystallization to the detriment of other forms.

1. Introduction

Scaling or fouling is a phenomenon in which originally dissolved mineral based salts are precipitated and cause blockage of fluid channels, condenser tubes and spacers or membrane surfaces. Build-up of a fouling film leads to an increase in resistance and deteriorates the performance of the process equipment such as membranes (Arras et al., 2009) and heat exchangers and is costing industries billions of dollars annually (Müller-Steinhagen, 2000). To mitigate scaling, it is very important ;to predict the scale propensity of feed water in order to modify and optimize the process accordingly.

Crystallization, particularly kinetic and thermodynamic aspects, has been studied for many years (Söhnel and Mullin, 1988; Mullin, 1993; Alimi and Elfil, 2003; Elfil and Roques 2001a; Elfil and Roques, 2004; Elfil and Hannachi, 2006; Elfil et al., 2007) and exhaustive material is available for pure salts, mainly calcium carbonate ($CaCO_3$) and calcium sulfate dehydrate ($CaSO_4 \cdot 2H_2O$) which are the major scaling contributors (Marshall and Slusher, 1966; Elfil and Roques 2001a, 2001b). In fact, recent studies have been interested to the possibility of controlling (Aleksandra, 2008; Wu et al., 2010) or reducing this problem by several methods, mainly chemical treatment (Aleksandra, 2008; Elfil et al., 2004). There are also a number of alternative non-chemical treatment options available. Amongst these is the use of magnetic, electronic and electrolytic treatment devices (MacAdam and Parsons, 2004; Al Nasser et al., 2011). Each of these scaling control methods has its own advantages and a number of factors

* Corresponding author. Tel./fax: +966 28082180.
E-mail addresses: noreddine.ghaffour@kaust.edu.sa (N. Ghaffour), h_elfil@yahoo.com (H. Elfil).

0009-2509/$ - see front matter © 2013 Elsevier Ltd. All rights reserved.
http://dx.doi.org/10.1016/j.ces.2013.03.028

need to be considered before selecting the right option. However, only few studies have been interested in mixed precipitation phenomenon, because of its complexity (Sheikholeslami and Sudmalis, 2000; 2003b). Therefore, not much attention has been paid to the interactive effect of co-precipitation of salts with and without common salt. This is mainly due to the difficulty of monitoring the mixed precipitation kinetics and the lack of thermodynamic data (Sheikholeslami, 2003a, 2003b).

Recent studies have shown that even the presence of small amount of another precipitating salt affects the thermodynamic and kinetics of precipitation and the scale structure as well (Sheikholeslami and Ng, 2001; Sheikholeslami, 2003a, 2003b). These investigations addressed the precipitation of one salt when another salt is present in a solid form and may act as a seed, may dissolve and contribute to the growth of the second salt, or may act as an adsorbent (Morse and Arakaki, 1993; Klepetsanis, 1995; Nancollas and Zieba, 1995). Therefore, the single salt data obtained under a single salt precipitation is not applicable to practical condition solutions.

This paper demonstrates the effect of $CaSO_4 \cdot 2H_2O$ on the structure and thermodynamic of $CaCO_3$ obtained in gypsum and $CaCO_3$ mixed precipitation phenomenon, which is commonly observed in industrial water treatment processes including thermal-based and membrane-based seawater desalination processes (Ghaffour et al., 2013; Gacem et al., 2012; Waly et al., 2012; Reddy and Ghaffour, 2007).

2. Background and theory

This paper looks at qualitative analysis of gypsum and $CaCO_3$ mixed precipitation from Kinetic and structural point of view. To simplify the result interpretation, general background of crystallization of pure $CaCO_3$, $CaSO_4 \cdot 2H_2O$ and mixed precipitation are briefly discussed in this section.

2.1. Crystallization mechanism

Crystallization is the formation of solid crystals precipitating in a solution. Crystallization process consists of two major steps: nucleation and crystal growth. Nucleation is the step where the solute molecules dispersed in the solvent start to gather into clusters, in nanometer scale, that becomes stable under the current operating conditions. These stable clusters constitute the nuclei. However, when the clusters are not stable they re-dissolve. Therefore, the clusters need to reach a critical size in order to become a stable nuclei. Such critical size is dictated by the operating conditions mainly temperature and supersaturation. It is at the stage of nucleation that the atoms are arranged in a defined and periodic manner that defines the crystal structure. On the other hand, the crystal growth is the subsequent growth of the nuclei that succeeds in achieving the critical cluster size.

Nucleation and growth continue to occur simultaneously while the supersaturation exists. Supersaturation is the driving force of crystallization; hence the rate of nucleation and growth are driven by the existing supersaturation in the solution. Once the supersaturation is exhausted, the solid–liquid system reaches equilibrium and the crystallization is completed unless the operating conditions are modified from equilibrium so that it will supersaturate the solution again.

2.2. Calcium carbonate and gypsum precipitation

Scaling, a frequent phenomenon in water distribution pipes, is characterized by the appearance of the packaging of an adhering crystalline deposit constituted essentially by $CaCO_3$ and $CaSO_4 \cdot 2H_2O$ on the pipe surfaces according to the following two reactions:

$$CO_2 + H_2O + CaCO_3 \leftrightarrows Ca(HCO_3)_2 \quad (1a)$$

$$HCO_3^- + H_2O \leftrightarrow CO_3^{2-} + H_3O^+ \quad (1b)$$

$$SO_4^{2-} + Ca^{2+} + 2H_2O \leftrightarrows CaSO_4 \cdot 2H_2O \quad (2)$$

All scaling processes by $CaCO_3$ result directly or indirectly from the first reaction (Eq.1). The CO_2 exchange between the liquid and gaseous phases is the main cause of any scaling. CO_2, in presence of a gaseous phase, can dissolve in the water. After hydration and ionization, CO_2 gives rise to an acid product which allows the attack of the present $CaCO_3$ in all the sedimentary rocks. Then it dissolves and passes in the solution in the form of hydrogenocarbonate which is much more soluble than the carbonate. This transformation (reaction from left to right in Eq. (1a)) corresponds to the sedimentary rocks solubilization process when the water is in contact with atmosphere rich in CO_2. If later this water loses the CO_2 by degassing and/or heating, the reaction can move to the other direction (reaction from right to left in Eq. (1a)) and gives rise to $CaCO_3$ scale. During $CaCO_3$ precipitation, calcium ions will react with carbonate (CO_3^{2-}) ions which accelerate the formation of H_3O^+ ions, as shown in Eq. (1b), leading to a pH decrease during germination.

Gypsum precipitation is less complex than $CaCO_3$ one. Indeed, it brings in only two phases (liquid and solid) all the phenomena governing the speed of the calcium sulfate to take place in the solution. The formation of this type of salt is not pH dependent and may occur in aqueous systems upon creation of conditions in which the solubility product is exceeded (Pavlo, 1991).

2.3. Mixed precipitation

Previous studies have shown that in case of mixed precipitation, the following two possibilities can exist (Morse and Arakaki, 1993; Sheikholeslami, 2003a, 2003b):

- The presence of a salt can affect the thermodynamics of the solution and afterward influences the other salt seeding kinetics.
- The salt obtained in a process of mixed precipitation can be present in different morphologies and crystalline structures from those obtained with the pure body's precipitation reactions.

3. Experimental procedure

3.1. Experimental unit

Mixed precipitation kinetics was studied carefully by monitoring four parameters simultaneously measured, that included: pH, calcium concentration [Ca^{2+}], alkalinity and quartz crystal microbalance (QCM) response. The experimental unit used to investigate the different parameters of $CaCO_3$ and gypsum mixed precipitation is represented in Fig. 1.

A thermostatic cell (1) of a capacity of 250 mL was used to maintain the solution at constant temperature by a thermostatic liquid circulation. The magnetic stirrer (2) was used to keep the solution homogeneous. The type of the used QCM was PM–720 Plating Monitor (3) equipped with a QCM electrode (4) that detect a very small mass (10^{-9} g) of precipitate deposited on its active surface. The solution pH was measured using Hanna Instrument HI 931401 pH meter (5). Two other apparatus were used to determine [Ca^{2+}] and alkalinity.

QCM is widely used to measure small changes in mass (about 10^{-9} g). Its operating principle is based on the variation of the resonant frequency of a quartz crystal with the mass of the

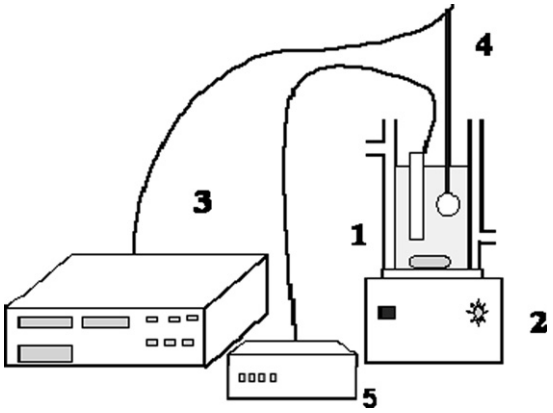

Fig. 1. Experimental unit, (1) Thermostatic cell, (2) Magnetic stirrer, (3) QCM, (4) QCM electrode, (5) pH meter.

deposited substances on its active surface (1 cm^2). The quartz is placed between two metal plates constituting the capacitor. When a potential difference is applied, the electrical field generated favors the crystal and an ultrasonic wave sound, whose length is inversely proportional to the resonant frequency of the quartz plate, is then created. The resonant frequency varies in proportion to the mass deposited in small amounts on one of the faces of the crystal (Elfil et al., 2004; Gabrielli et al., 1991).

3.2. Solution preparation

Solutions were prepared with double decomposition method using two solutions of sodium sulfate (Na_2SO_4), sodium bicarbonate ($Na \cdot HCO_3$) and calcium chloride ($CaCl_2$). Ionic strength was fixed at 0.5 M using sodium chloride. This method is mainly used to reach high supersaturations. In contrast to the dynamic methods where supersaturation is gradually decreased up to precipitation, the double decomposition allows only for a specified supersaturation to observe or not the precipitation. It is important to notice that the concentration of the different ions must be higher than that corresponding to the precipitation edge which is limited, in the case of calco-carbonic system, to the solubility of the monohydrated form.

Estimation of ionic activity coefficient was useful to determine the two salts precipitation and supersaturation. Pitzer simplified model was used to calculate all the activity coefficients (Pitzer and Mayorga, 1974).

Supersaturation Ω is defined as the ionic activity product and the solubility product ratio:

$$\Omega = IAP/\,Ks \tag{3}$$

Supersaturation was calculated as follow:

For the $CaCO_3$:

$$\Omega/_{CaCO_3} = \frac{(Ca^{2+})(CO_3^{2-})}{Ks/CaCO_3} \tag{4}$$

$$\Omega/_{CaCO_3} = \frac{[Ca^{2+}]\gamma_{Ca^{2+}}[CO_3^{2-}]\gamma_{CO_3^{2-}}10^{pH-pK_2}}{Ks/_{CaCO_3}} \tag{5}$$

For the gypsum:

$$\Omega/_{Gypsum} = \frac{(Ca^{2+})(SO_4^{2-})}{Ks/_{Gypsum}} \tag{6}$$

$$\Omega/_{Gypsum} = \frac{[Ca^{2+}]\gamma_{Ca^{2+}}[SO_4^{2-}]\gamma_{SO_4^{2-}}}{Ks/_{Gypsum}} \tag{7}$$

where Ω is the supersaturation, IAP is the Ionic Activity Product, [ ] is the molar concentration, *Ks* is the solubility constant, ( ) is the activity, γ is the ionic activity coefficient and K_2 is the constant of $CaCO_3$ second ionization.

For $T=30\,^{\circ}C$: $Ks/_{Gypsum} = 4.25 \times 10^{-5}$ (Marshall and Slusher, 1966) and $Ks/_{CaCO_3\ (calcite)} = 3.1 \times 10^{-9}$ (Bischoff et al., 1993).

Calcium concentration and alkalinity were determined throughout the experiment using volumetric dosages.

- pH and alkalinity (Alk) were used to follow the $CaCO_3$ precipitation.
- Calcium concentration was mainly used to follow the gypsum germination.
- QCM response was used to follow the two salts precipitation especially gypsum (Elfil et al., 2004; Abdel-Aal et al., 2002).

These parameters allowed us to detect the $CaCO_3$ and gypsum precipitations. In fact, during $CaCO_3$ germination, pH and total alkalinity decreased simultaneously because the concentration of carbonate in the solution is pH dependent and the pH of the solution changes during the run due to the fact that carbonate is depleting by precipitation, while calcium concentration did not decrease considerably. Because gypsum solubility is much higher than that of $CaCO_3$, one has to conclude that the calcium concentration decreases correspond to $CaCO_3$ germination which is negligible compared to $CaSO_4 \cdot 2H_2O$ one. Therefore, during gypsum precipitation, as pH and total alkalinity remained constant because $CaSO_4$ germination is pH independent, calcium concentration decreased.

The QCM detected with precision $CaCO_3$ and $CaSO_4 \cdot 2H_2O$ precipitations. It characterizes $CaCO_3$ precipitation when it is accompanied with pH and total alkalinity drop and gypsum germination when it is accompanied with calcium concentration decrease.

Scanning electron microscopy (SEM) was used to identify the nature of the precipitates and to confirm the electro microscopic results.

4. Results and discussion

A comparison of $CaCO_3$ and $CaSO_4 \cdot 2H_2O$ mixed precipitation results of both cases, when $CaCO_3$ precipitation occurs first and when gypsum precipitation occurs first, is presented from a kinetics and structural point of view.

4.1. Case 1: CaCO3 germination followed by gypsum precipitation

Fig. 2a shows two phenomena. The first one is the pH and alkalinity decrease characterizing $CaCO_3$ germination, and the second one is the considerable decrease of calcium concentration characterizing $CaSO_4 \cdot 2H_2O$ germination. On the other hand, Fig. 2b shows that QCM detected with precision the seed precipitation. The first response characterizes $CaCO_3$ precipitation because it is accompanied with pH and alkalinity drop and the second one characterizes gypsum germination which is accompanied with the important decrease of calcium concentration.

4.1.1. Scale structure

To identify the nature of the deposit collected after the first and the second precipitation, samples were analyzed using high resolution SEM images. The structure of the tow salts is represented in Fig. 3.

In the case of $CaCO_3$ precipitation followed by gypsum germination, the deposit collected after the first precipitation is shown in Fig. 3a. $CaCO_3$ scale had hexagonal structure of vaterite

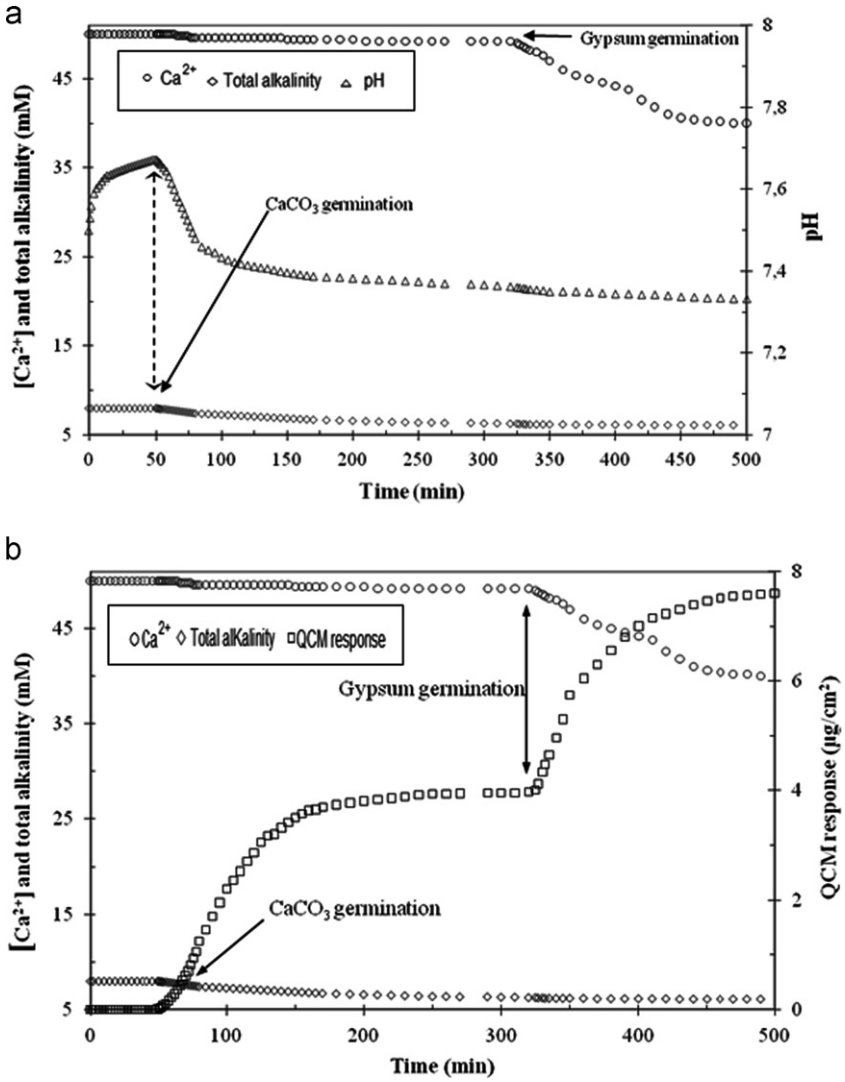

Fig. 2. (a) Calcium concentration, total alkalinity and pH *vs* time at 30 °C (Case 1), ($[Ca^{2+}]_i$=50 mM; $[Alk]_i$=8 mM; $[SO_4^{2-}]_i$=30 mM), (b) QCM response, total alkalinity and calcium concentration *vs* time at 30 °C (Case 1), ($[Ca^{2+}]_i$=50 mM; $[Alk]_i$=8 mM; $[SO_4^{2-}]_i$=30 mM).

characterized by a soil rose form. After gypsum precipitation, the deposit collected which is a mixture of $CaCO_3$ and calcium sulfate is shown in Fig. 3b. The scale from the co-precipitation is a mixture of gypsum crystalized in a monoclinic system and $CaCO_3$ having vaterite form. The presence of $CaCO_3$ crystals in the solution did not have significant effect on $CaSO_4$ germination.

4.2. Case 2: gypsum germination followed by $CaCO_3$ precipitation

Figs. 4a and b show that QCM response is only accompanied with calcium concentration drop characterizing gypsum precipitation. In this case it did not give any information about $CaCO_3$ precipitation. Ten minutes after gypsum germination, the alkalinity declined accompanied by a pH drop characterizing $CaCO_3$ precipitation. The short time between the two precipitations allow us to think about dependence between $CaCO_3$ and gypsum germinations. It is suggested that pH is the principal parameter indicating the $CaCO_3$ germination.

4.2.1. Scale structure

In the case of gypsum germination followed by $CaCO_3$ precipitation, the deposit collected after the first precipitation, which is shown in Fig. 5a, is constituted only by gypsum crystals. In a second step, when $CaCO_3$ precipitation occurred, the deposit collected which is a mixture of $CaCO_3$ and calcium sulfate is presented in Fig. 5b. The co-precipitation scale is a mixture of gypsum and $CaCO_3$ in its calcite form. The calcite is crystallized in rhombohedra system (Elfil and Roques 2001a, 2001b). The absence of vaterite, contrary to the first case, suggests the hypothesis that gypsum crystals promoted $CaCO_3$ crystallization especially calcite form.

4.3. Study of calcium ions influence

Calcium ions contribute to both precipitation structures. It is a common ion in $CaCO_3$ and gypsum formation. That is why it is important to study its influence on the germination of the two salts.

The germination time of gypsum and $CaCO_3$ for different sulfate ions concentrations varying from 40 mM to 80 mM versus calcium concentration is presented in Figs. 6a and b, respectively.

In the case of gypsum germination (Fig. 6a), we observed firstly that for the same sulfate ions concentration, gypsum germination time is inversely proportional to the calcium ions concentration for all sulfate concentrations. However, the influence of calcium concentration on gypsum germination time is more significant for

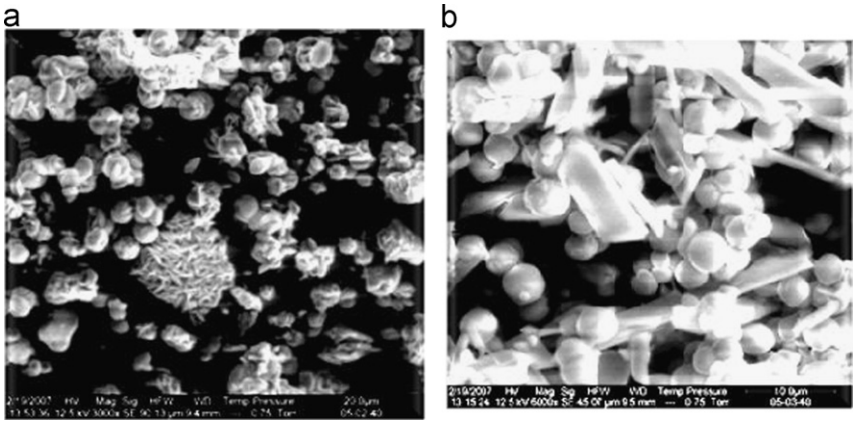

Fig. 3. SEM photos of the first and the second precipitates when $CaCO_3$ precipitation occurred first, (a) vaterite salt precipitate, (b) (vaterite+gypsum) salt precipitate (Case 1).

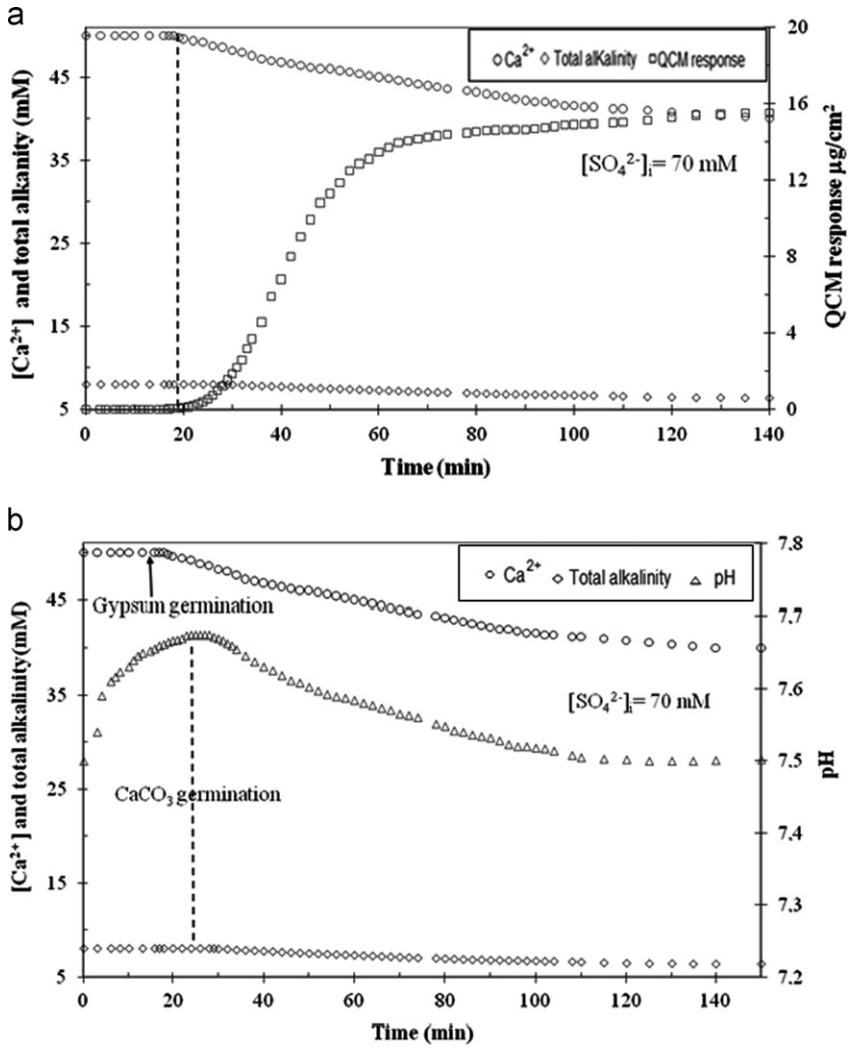

Fig. 4. (a) QCM response, total alkalinity and calcium concentration *vs* time at 30 °C (Case 2), ($[Ca^{2+}]_i$=50 mM; $[Alk]_i$=8 mM; $[SO_4^{2-}]_i$=70 mM).(b) Calcium concentration, total alkalinity and pH *vs* time at 30 °C (Case 2), ($[Ca^{2+}]_i$=50 mM; $[Alk]_i$=8 mM; $[SO_4^{2-}]_i$=70 mM).

the high sulfate ions concentration. On the other hand, in Fig. 6b, we observe the same effect of calcium influence for all sulfate ions concentrations. Here also, the $CaCO_3$ germination time is widely decreasing by the increase of calcium concentration thought that a limit was found for sulfate concentrations of 50 mM above which the influence was less.

To better understand this behavior, $CaCO_3$ germination time versus sulfate ions concentration at different calcium concentrations varying from 50 mM to 80 mM was studied. Results presented in Fig. 6c show that a maximum germination time peak was found at a concentration of 40 mM of sulfate ions for all tested calcium concentrations. The peak was reduced from 220 min to 10 min by

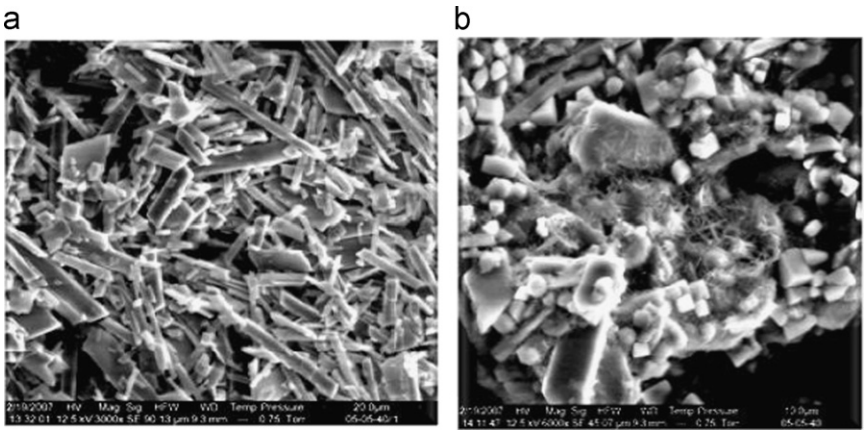

Fig. 5. SEM photos of the first and the second precipitate when calcium sulfate precipitation occurred first, (a) gypsum precipitate (b) gypsum and calcite precipitate (Case 2).

increasing calcium concentration from 50 mM to 80 mM, respectively. The same phenomenon was observed for sulfate ion concentration below 40 mM but with lower amplitude. The $CaCO_3$ germination seems to be influenced by the $CaSO_4 \cdot 2H_2O$ system.

4.4. Study of bicarbonate ions influence

In the case where $CaCO_3$ crystals appear first, increasing the initial bicarbonate ions concentration increases $CaCO_3$ supersaturation and consequently the germination time is reduced. In this case $CaCO_3$ precipitation is only related to the supersaturation. This is confirmed by experimental results presented in Fig. 7a. On the other hand, in the case where gypsum precipitates first, germination time of the seed precipitates and $CaCO_3$ supersaturation versus bicarbonate concentration, presented in Fig. 7b, shows that $CaCO_3$ germination time remains almost constant while the supersaturation is increasing. $CaCO_3$ germination time seems to be related to gypsum germination and not anymore to the supersaturation as in a simple homogenous germination.

4.5. $CaCO_3$ and sulfate precipitation fields

In order to better understand the process and obtain deeper explanation of the germination time of the two salts, gypsum and $CaCO_3$ germination time and $CaCO_3$ supersaturation versus sulfate ions concentration for $[Ca^{2+}]_i = 50$ mM and $[Alk]_i = 8$ mM were investigated.

In contrast to the classical evolution of the gypsum germination time which is proportional to its supersaturation, the $CaCO_3$ germination time can be divided in two fields as shown in Fig. 8. In the field A, $CaCO_3$ spontaneous precipitation appears first and $CaCO_3$ germination time is inversely proportional to the supersaturation. However, in the field B, when gypsum germination begins first, the $CaCO_3$ precipitation occurs independently of the supersaturation. The germination time deceases although $CaCO_3$ supersaturation decreases which is in contradiction with the homogenous germination thermodynamic and kinetic rules. These rules seem to be broken by the presence of $CaSO_4 \cdot 2H_2O$ crystals derived from gypsum germination when the latter precipitates first. In fact, few minutes after gypsum germination, $CaCO_3$ precipitation is induced independently to supersaturation. This phenomenon is repeated every time when the gypsum germination occurs first in a saturated calco-carbonic solution. Gypsum crystals seem playing a precursor role on $CaCO_3$ precipitation.

4.6. Study of gypsum crystals influence in $CaCO_3$ precipitation

To confirm the role of gypsum crystals as precursor in the $CaCO_3$ germination, a series of experiments were performed. Experiments where $CaCO_3$ precipitation occurred first were repeated with injection of a small quantity of gypsum crystals (0.2–0.5 g/L) before the $CaCO_3$ spontaneous germination. The resuts of this investigation are represented in Fig. 9.

It is important to notice that the solutions were slightly supersaturated with regard to gypsum, therefore the risk of gypsum partial dissolution, which could increase the calcium concentration, does not exist.

We observed that the pH and the total alkalinity dropped in the same time with gypsum injection. In fact without gypsum injection, $CaCO_3$ germination occurred at 35 min. However, the injection of small quantities of gypsum at 8 and 20 min, respectively, promote immediately $CaCO_3$ precipitation, as shown in Fig. 9.

These results confirm that the crystals of gypsum behave as a precursor of a heterogeneous seeding of $CaCO_3$. The presence of gypsum crystals seem to reduce the $CaCO_3$ energetic barrier and lead its precipitation especially calcite toward other forms. In fact, previous studies have demonstrated that in the case of mixed precipitation, two possibilities can exist:

1. The presence of a salt can affect the thermodynamics of the solution and afterward influence the other salt seeding kinetics (Sheikholeslami and Sudmalis, 2000). In fact, the thermodynamic solubility constant of pure salt precipitation is different from that of co-precipitation due to the fact that the product of co-precipitation differs from that of single salt precipitation. Based on thermodynamic principals, it is hypnotized that this is related to the change in standard molar Gibbs free energy of reaction (Sheikholeslami and Ng, 2001).
2. The salt obtained in a process of mixed precipitation can present different morphologies and crystalline structures from those obtained with the pure body's precipitation reactions (Sheikholeslami and Sudmalis, 2000). In fact, studies where the crystal of co-precipitated $CaCO_3$ and sulfate crystals were examined have shown that pure calcium sulfate deposit was found to be far less adherent then deposits containing co-precipitated $CaCO_3$. The latter seems to act as bonding cement, enhancing considerably the strength of calcium scale layer (Sheikholeslami and Sudmalis, 2000). However, in presence of $CaSO_4$, the $CaCO_3$ scale which is usually very adherent and tenacious loses its strength and becomes less adherent and more freely moving (Sheikholeslami, 2003a, 2003b).

To determine the obtained precipitate morphology, IR spectroscopy identification of the deposit collected 10 min after the gypsum injection shows, by comparing with the peaks corresponding to pure gypsum used for seeding, the presence of peaks corresponding to calcite crystals (Fig. 10).

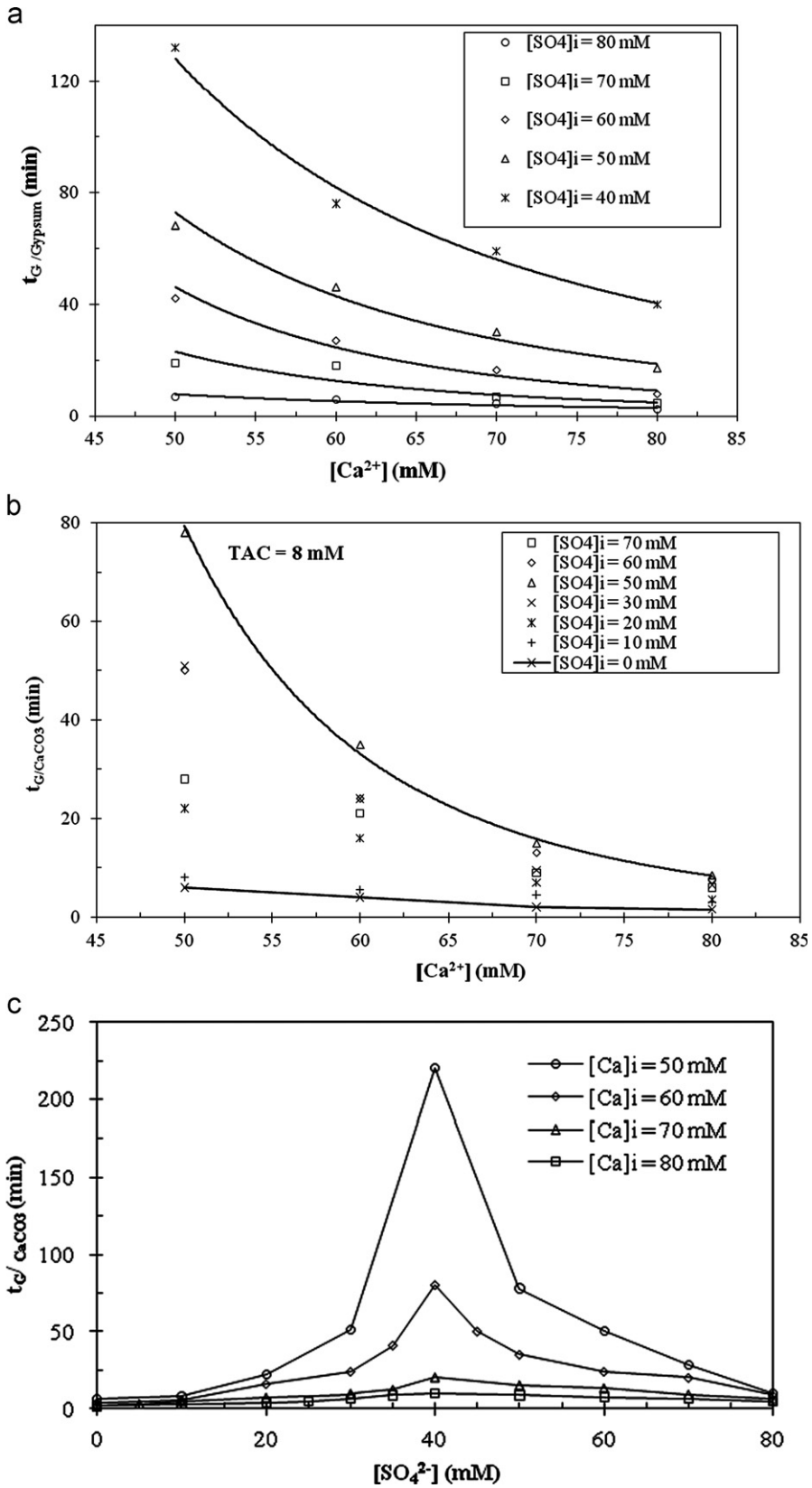

Fig. 6. (a) Gypsum germination time *vs* [ca^{2+}] for different sulfate ions concentrations, ([Alk]$_i$=8 mM). (b) $CaCO_3$ germination time *vs* [ca^{2+}] for different sulfate ions concentrations, ([Alk]$_i$=8 mM). (c) $CaCO_3$ germination time *vs* sulfate ions concentration for different calcium concentrations, ([Alk]$_i$=8 mM).

The presence of gypsum crystals plays the role of a precursor which induced $CaCO_3$ precipitation. In fact, in $CaCO_3$ simple precipitation, the vaterite is the predominant precipitate form while when it comes to $CaCO_3$ mixed precipitation the calcite is the dominant one.

5. Conclusions

To study $CaCO_3$ and sulfate mixed precipitation, four parameters were investigated simultaneously: pH and Alkalinity to

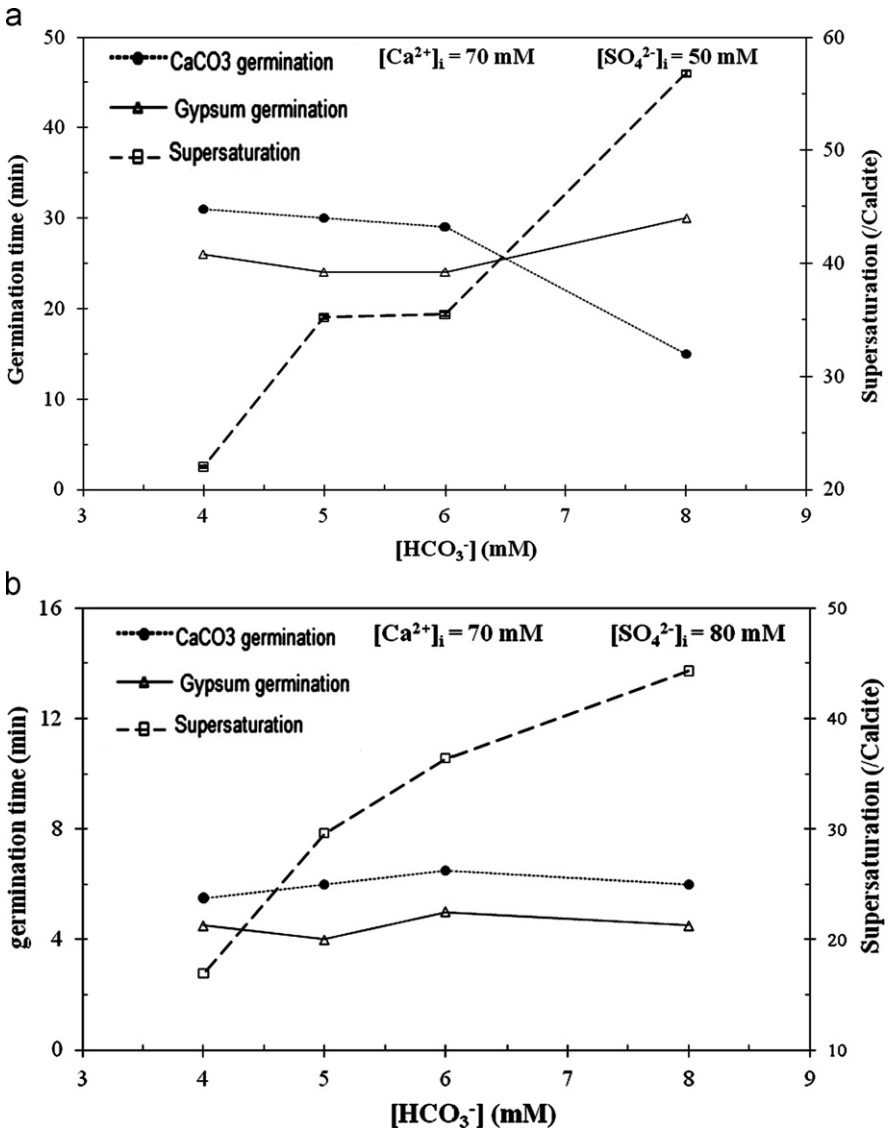

Fig. 7. (a) Germination time of the tow precipitates and $CaCO_3$ supersaturation *vs* bicarbonate ions concentration when $CaCO_3$ germination occurs first, ($[Ca^{2+}]_i$= 70 mM; $[SO_4^{2-}]_i$=50 mM). (b) Germination time of the tow precipitates and $CaCO_3$ supersaturation *vs* bicarbonate ions concentration when gypsum germination occurs first, ($[Ca^{2+}]_i$=70 mM; $[SO_4^{2-}]_i$=80 mM).

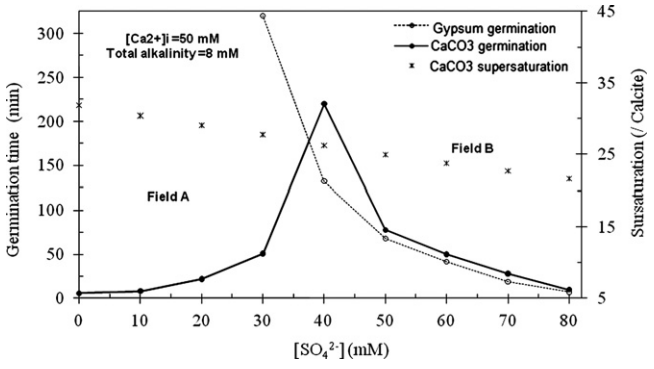

Fig. 8. Gypsum germination time, $CaCO_3$ germination time and $CaCO_3$ supersaturation *vs* sulfate ions concentration, ($[Ca^{2+}]_i$=50 mM; $[HCO_3^-]_i$=8 mM).

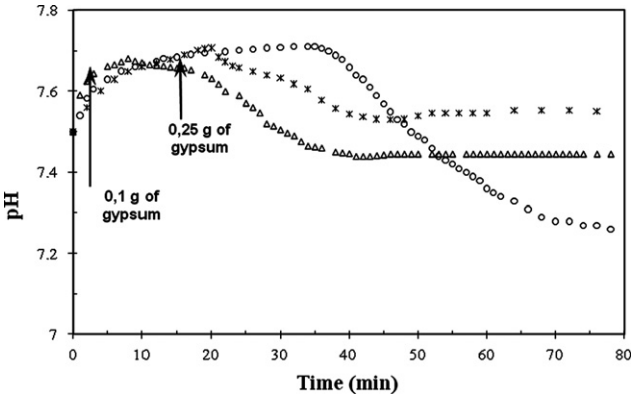

Fig. 9. pH evolution with and without gypsum injection, ($[Ca^{2+}]_i$=60 mM; $[HCO_3^-]_i$=8 mM; $[SO_4^{2-}]_i$=50 mM).

follow the $CaCO_3$ germination, calcium concentration characterizing gypsum precipitation and the QCM response that detect the seed precipitations.

The influence of co-precipitation ions was studied and results showed that an increase of calcium ion (common ions for the tow precipitation) concentration leads to the germination of the two salts. On the other hand, an increase of sulfate ion concentration reduces considerably the gypsum germination time and affects the $CaCO_3$ induction time evolution.

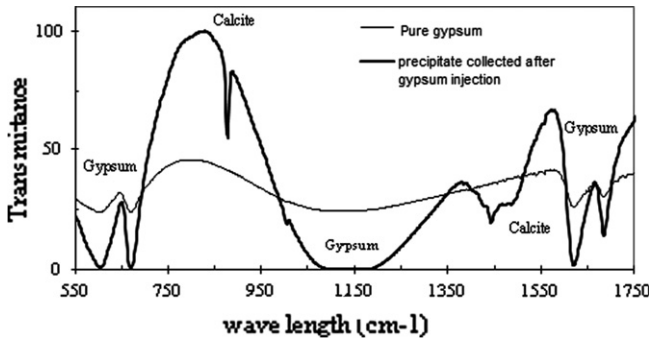

Fig. 10. IR identification of the precipitate collected after gypsum injection.

Furthermore, results showed that when the sulfate concentration is higher than 40 mM, (for the case when gypsum precipitation begins first), the $CaCO_3$ germination starts immediately and is not anymore related to the supersaturation as in a simple homogenous precipitation. In fact, previous studies investigating the effect of the presence of sulfate ions on the precipitation of $CaCO_3$ have shown that the solubility of $CaCO_3$ increases with an increase in sulfate ions, but it appears to limit the effect of $CaSO_4$ on $CaCO_3$ precipitation (Sheikholeslami and Ng, 2001). To compare this finding to ours, $CaCO_3$ precipitation kinetics were investigated in a calco-carbonic solution in the absence and presence of gypsum. It was found that the pH and the total alkalinity decreased immediately after gypsum injection, which herein confirms that the presence of $CaSO_4.2H_2O$ crystals enhances $CaCO_3$ germination. Here the gypsum crystals behave as the precursor of a heterogeneous seeding of $CaCO_3$. The presence of gypsum crystals seems to reduce the $CaCO_3$ energetic barrier and leads to precipitation in calcite form by activating its heterogeneous germination.

$CaCO_3$ germination, in the presence of the gypsum process, evolved into a different form that was found in the case of simple precipitation. However, $CaCO_3$ crystals formation was shown to not have any significant effect on gypsum precipitation.

References

Abdel-Aal, N., Satoh, K., Sawada, K., 2002. Study of the adhesion mechanism of $CaCO_3$ using a combined bulk chemistry/QCM technique. J. Cryst. Growth 245, 87–100.

Aleksandra, S., 2008. Influence of SDS on particle size and adhesionof precipitating calcium carbonate. Colloids Surfaces A: Physicochem., Eng. Aspects 320, 98.

Alimi, F., Elfil, H., 2003. Kinetics of precipitation of calcium sulfate dehydrate in desalination unit. Desalination 158, 9–16.

Al Nasser, W.N., Al Ruwaie, A.H., Hounslow, M.J., Salman, A.D., 2011. Influence of electronic antifouling on agglomeration of calcium carbonate. Powder Technol. 206, 201.

Arras, W., Ghaffour, N., Hamou, A., 2009. Performance evaluation of BWRO desalination plant—a case study. Desalination 235, 170–178.

Bischoff, J.L., Fitzatrick, J.A., Rosenbuer, R.J., 1993. The solubility and stabilization of Ikaïte ($CaCO_3 \cdot 6H_2O$) from 0 to 25 °C: environmental and paleoclimatic implications for thinolite Tufa. J. Geol. 101, 21.

Elfil, H., Hamed, A., Hannachi, A., 2007. Technical evaluation of a small-scale reverse osmosis desalination unit for domestic water. Desalination 203 (319), 326.

Elfil, H., Hannachi, A., 2006. Reconsidering water scaling tendency assessment. AIChe J. 52, 3583–3591.

Elfil, H., Nawel, R., Gadri, A., Bolliger, J.C., 2004. Chemical inhibition of gypsum precipitation at 30 using quartz crystal microbalance. Eur. J. Hydrol.35, 161–176.

Elfil, H., Roques, H., 2001a. Role of hydrate phases of calcium carbonate 392 on the scaling phenomenon. Desalination 137, 177–186.

Elfil, H., Roque, H., 2004. Prediction of the limit of the metastable zone in the "$CaCO_3$–CO_2–H_2O". AIChE J. 50, 1908–1916.

Elfil, H., Roques, H., 2001b. Rôle de la microbalance à quartz dans l'étude de germination du carbonate de calcium. Entropie 231, 28.

Gabrielli, C., Keddam, M., Torresi, R., 1991. Calibration of the electrochemical quartz microbalance. J. Electrochem. Soc. 138, 2657–2660.

Gacem, Y., Taleb, S., Ramdani, A., Senadjki, S., Ghaffour, N., 2012. Physical and chemical assessment of MSF distillate and SWRO product for drinking purpose. Desalination 290, 107–114.

Ghaffour, N., Missimer, T.M., Amy, G.L., 2013. Technical review and evaluation of the economics of water desalination: current and future challenges for better water supply sustainability. Desalination 309, 197–207.

Klepetsanis, P.G., 1995. The calcite–hydroxypatite system. In: Amjad, Z. (Ed.), Crystal Growth Studies in Aqueous Solution, in Mineral Scale Formation and Inhibition. Plenum Press, New York, pp. 251.

MacAdam, J., Parsons, S.A., 2004. Calcium carbonate scale formation and control. Rev. Environ. Sci. Biotechnol. 3, 159–169.

Marshall, W.L., Slusher, R., 1966. Thermodynamics of calcium sulfate dehydrate in aqueous sodium chloride solution, 0–100 °C. J. Phys. Chem. 70, 4015.

Morse, J., Arakaki, T., 1993. Adsorption and co-precipitation of divalent metals with mackinawite. Cosmochim. Acta 57, 3635.

Mullin, J.W., 1993. Crystallization, 3rd 410 edition Butterworth-Heinemann, London.

Müller-Steinhagen, H., 2000. On Line Cleaning Methods: Heat Exchanger Fooling, Mitigation and Cleaning Technologies. Publ. Institution of chemical Engineers, UK.

Nancollas, G.H., Zieba, A., 1995. Constant composition kinetics studies of the simultaneous crystal growth of alkaline earth carbonates and phosphates. In: Amjad, Z. (Ed.), In Mineral Scale Formation. Plenum Press, New York, pp. 1.

Pavlo, G., 1991. Spontaneous precipitation of calcium sulfate at conditions of sustained supersaturation. J. Colloid Interface Sci. 143, 299.

Pitzer, K.S., Mayorga, G., 1974. Thermodynamics of electrolyte. III. Activity and osmotic coefficients for 2-2 electrolytes. J. Solution Chem. 3, 539–546.

Reddy, K.V., Ghaffour, N., 2007. Overview of the cost of desalinated water and costing methodologies. Desalination 205, 340–353.

Sheikholeslami, R., 2003a. Nucleation and kinetics of mixed salts in scaling. AIChE J. 49, 193–194.

Sheikholeslami, R., 2003b. Mixed salts-scaling limits and propensity. Desalination 154, 117.

Sheikholeslami, R., Ng, M., 2001. Calcium sulfate precipitation in the 425 presence of non-dominant calcium carbonate: thermodynamics and kinetics. Ind. Eng. Chem. Res. 40, 3570.

Sheikholeslami, R., Sudmalis, M., 2000. Coprecipitation of $CaCO_3$ and $CaSO_4$. Can. J. Chem. Eng. 78, 21–22.

Söhnel, O., Mullin, J.W., 1988. Interpretation of crystallization induction periods. J. Colloid Interface Sci. 123, 43.

Waly, T., Kennedy, M.D., Witkamp, G.J., Amy, G., Schippers, J.C., 2012. The role of inorganic ions in the calcium carbonate scaling of seawater reverse osmosis systems. Desalination 284, 279–287.

Wu, Z., Davidson, J.H., Francis, L.F., 2010. Effect of water chemistry on calcium carbonate deposition on metal and polymer surfaces. J. Colloid Interface Sci. 343, 176.